ELSEVIER

Biochimica et Biophysica Acta 1429 (1999) 486–495

BIOCHIMICA ET BIOPHYSICA ACTA
BBA

Dynamic equilibrium unfolding pathway of human tumor necrosis factor-α induced by guanidine hydrochloride

Yong-Rok Kim [a,*], Joong-Sik Hahn [a], Heedeok Hong [a], Woojin Jeong [b], Nam Woong Song [c], Hang-Cheol Shin [1,b], Dongho Kim [1,c]

[a] *Department of Chemistry, Yonsei University, Shinchon-Dong 134, Seodaemun-Gu, Seoul 120-749, South Korea*
[b] *Hanhyo Institute of Technology, 461-6 Chunmin Dong, Yusung Ku, Taejon 305-390, South Korea*
[c] *National Creative Research Initiatives Centre for Ultrafast Optical Characteristics Control and Spectroscopy Laboratory, Korea Research Institute of Standards and Science, P.O. Box 102, Yusung Ku, Taejon 305-600, South Korea*

Received 16 July 1998; received in revised form 9 October 1998; accepted 19 November 1998

Abstract

The dynamic equilibrium unfolding pathway of human tumor necrosis factor-α (TNF-α) during denaturation at different guanidine hydrochloride (GdnHCl) concentrations (0–4.2 M) was investigated by steady-state fluorescence spectroscopy, potassium iodide (KI) fluorescence quenching, far-UV circular dichroism (CD), picosecond time-resolved fluorescence lifetime, and anisotropy decay measurements. We utilized the intrinsic fluorescence of Trp-28 and Trp-114 to characterize the conformational changes involved in the equilibrium unfolding pathway. The detailed unfolding pathway under equilibrium conditions was discussed with respect to motional dynamics and partially folded structures. At 0–0.9 M [GdnHCl], the rotational correlation times of 22–25 ns were obtained from fluorescence anisotropy decay measurements and assigned to those of trimeric states by hydrodynamic calculation. In this range, the solvent accessibility of Trp residues increased with increasing [GdnHCl], suggesting the slight expansion of the trimeric structure. At 1.2–2.1 M [GdnHCl], the enhanced solvent accessibility and the rotational degree of freedom of Trp residues were observed, implying the loosening of the internal structure. In this [GdnHCl] region, TNF-α was thought to be in soluble aggregates having distinct conformational characteristics from a native (N) or fully unfolded state (U). At 4.2 M [GdnHCl], TNF-α unfolded to a U-state. From these results, the equilibrium unfolding pathway of TNF-α, trimeric and all β-sheet protein, could not be viewed from the simple two state model (N → U).

Keywords: Human tumor necrosis factor-α; Equilibrium unfolding; Tryptophan; Fluorescence spectroscopy; Motional dynamics

1. Introduction

Understanding the protein folding pathway is one of the interesting fields in physical chemistry when intact proteins are used in the laboratory since folding is a self-assembly process that occurs spontaneously under the appropriate conditions, directed by physical interactions with the solvent and between different parts of the protein [1]. The protein folding study has attracted wide attention in recent years because it helps in understanding the intermediates involved in the folding pathways [2–4]. In particular,

* Corresponding author. Fax: +82 (2) 364-7050; E-mail: yrkim@alchemy.yonsei.ac.kr
[1] Also corresponding authors.
H.-C.S., Fax: +82 (42) 866-9129; hcshin@donald.hanhyo.co.kr.
D.K., Fax: +82 (42) 868-5027; dongho@krissol.kriss.re.kr

0167-4838/99/$ – see front matter
PII: S0167-4838(98)00263-5

tumor necrosis factor-α (TNF-α) is a cytokine which is believed to play an important role in a wide range of cell regulatory, immune, and inflammatory properties [5–7]. In addition, it is ideal for folding studies because of its interesting trimeric native structure and all β-sheet property [8–10]. For these reasons, TNF-α has been extensively investigated with regard to its structure, thermodynamics, and kinetics of folding [11–14].

Many relevant studies of protein folding used guanidine hydrochloride (GdnHCl) and urea as the most common denaturants for studies of protein stability, unfolding, and refolding [3,4]. The unfolded states of proteins such as carbonic anhydrase staphylococcal nuclease, pGSTP1-1, barstar, PGK, and IGPS were monitored under the equilibrium conditions using different guanidine hydrochloride concentrations [15–21], while there exists only a little information about the conformation of TNF-α which is induced by GdnHCl rather than by acid or temperature.

The fluorescence technique that we adapted in this work has been extensively used in characterizing the structural and dynamic aspects of many proteins [22–24]. Steady-state fluorescence spectra of optically isolated tryptophans can reflect the polarities of their surrounding environments. In addition, the quenching of tryptophan fluorescence by several chemical species has also become a powerful tool for studying the location of Trp residues in the protein matrix, particularly their dynamic exposure to the solvent. Ionic quenchers, due to their charges and strongly hydrated characteristics, can extinguish only the fluorescence emitted by fluorophores located at or near the surface of the protein [22,25]. In particular, since the time-resolved fluorescence anisotropy decay gives valuable insights into the local structure around the tryptophan residues as well as the tumbling motion for the whole protein, many studies have been performed on picosecond or nanosecond time scales that include the motional dynamics of the proteins [22–24].

In the present work, we have studied the conformation of human TNF-α in various GdnHCl concentrations by steady-state fluorescence, picosecond time-resolved fluorescence lifetimes, and anisotropy decays. In this paper, we report the first picosecond time-resolved measurements for the internal motion during the GdnHCl-induced unfolding of human TNF-α. In addition, we suggest the presence of the loosely packed and aggregated intermediates with very different spectroscopic and hydrodynamic properties from those of native and fully unfolded forms.

2. Materials and methods

2.1. Materials

Protein solutions were incubated for 24 h at ambient temperature in a 50 mM sodium phosphate buffer (pH 7.6) containing the desired concentration (0–4.2 M) of GdnHCl to ensure that equilibrium had been reached. Protein concentrations were about 0.125 mg/ml (2.40 μM as trimer) for steady-state, time-resolved fluorescence measurements. Human TNF-α was supplied by the Hanhyo Institute of Technology, and all the chemicals used in the experiments were of analytical grade.

2.2. Steady-state fluorescence and far-UV CD measurements

Tryptophan fluorescence spectra in both the absence and the presence of the quencher were measured using a fluorescence spectrophotometer (Hitachi F-4500). Emission spectra were recorded over 250–550 nm using an excitation wavelength of 295 nm in order to avoid the complications arising from multiple emitters. The excitation and emission bandwidths were both 10 nm. Far-UV CD measurements were carried out using a Jasco J-710 spectropolarimeter. All spectra were collected at ambient temperature.

2.3. Picosecond time-resolved fluorescence lifetime and anisotropy decay measurements

Time-resolved fluorescence decays of human TNF-α were measured by employing a picosecond time-correlated single photon counting (TCSPC) system. TCSPC laser system utilized in this study consisted of a cavity-dumped dye laser which was synchronously pumped by a mode-locked argon ion laser. The laser output from the cavity dumped dye laser was frequency-doubled by BBO crystal to obtain the excitation wavelength of 295 nm. The 310- nm cut-off filter was used in order to prevent the scattered

light from entering the monochromator. The temporal pulse width of the excitation beam and the FWHM of the instrumental response function were 2–3 ps and about 60 ps, respectively. More detailed information on this TCSPC system was reported in the previous publication [26]. The data collection time was minimized to 200 s in order to avoid any thermal denaturation by irradiation. Detection wavelengths were 330 or 350 nm. The vertical and the horizontal components of fluorescence emission were simultaneously fitted to extract the anisotropy decay functions using the LIFETIME program with an iterative nonlinear least-squares deconvolution procedure developed at the University of Pennsylvania. The fluorescence intensity decay curves were all fitted by triple exponentials, and the anisotropy decay curves were fitted by single or double exponentials. The fitted results of the fluorescence lifetime measurements were used to evaluate the mean lifetimes ($\tau_m = \Sigma\alpha_i\tau_i/(\Sigma\alpha_i)$), which were incorporated into the KI fluorescence quenching results. The protein concentrations and solution conditions were the same as for the steady-state measurements.

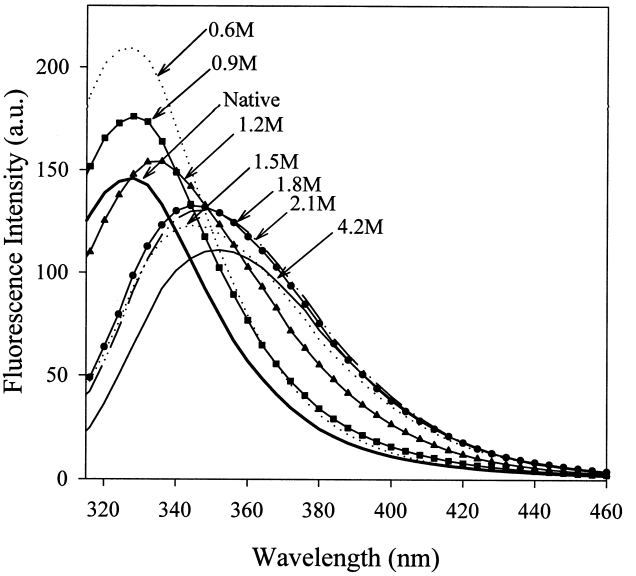

Fig. 1. Steady-state fluorescence emission spectra of human TNF-α were in aqueous phosphate buffer solutions of pH 7.6 at various GdnHCl concentrations. Excitation wavelength was 295 nm. Each protein concentration was 0.125 mg/ml.

3. Results and discussion

3.1. Steady-state fluorescence and lifetime measurements

As shown in Fig. 1, the steady-state fluorescence spectra of human TNF-α with different GdnHCl concentrations appeared in the wavelength range of 310–460 nm. Analysis of the spectra showed that tryptophanyl environments were strongly dependent upon the concentration of GdnHCl. Overall, the fluorescence spectral maximum shift from 328 to 352 nm is due to the changes in solvent accessibility of the hydrophobic tryptophan residues, and these phenomena were demonstrated in the previous

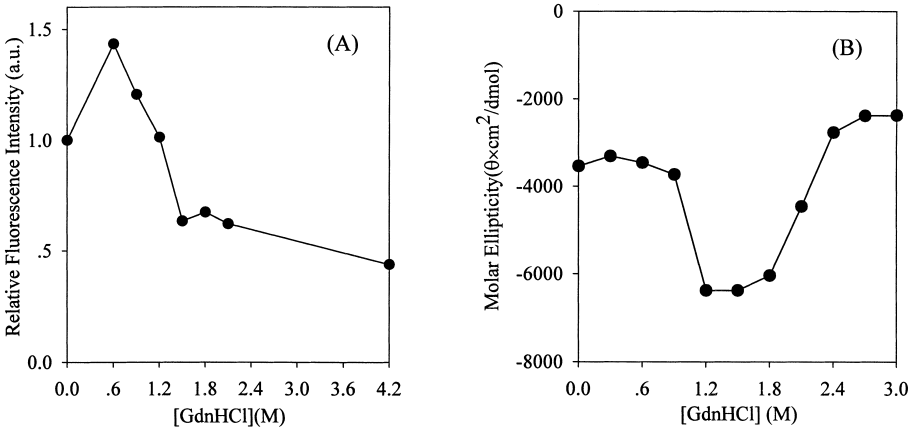

Fig. 2. GdnHCl-induced unfolding transitions were monitored by (A) the fluorescence intensity at the emission wavelength of 328 nm by 295 nm excitation and (B) the far-UV circular dichroism at 220 nm as a function of GdnHCl concentration in 50 mM sodium phosphate buffer of pH 7.6. Other experimental conditions are described in Section 2.2.

publication for the GdnHCl (6 M)-induced denatured equilibrium state of TNF-α [11].

In Fig. 2A, the unfolding transition curve monitored by Trp fluorescence excited at 295 nm shows that there is a large increase in fluorescence intensity by about 50% of native fluorescence up to 0.6 M [GdnHCl] and then a gradual decrease to about 40% of the native fluorescence at 4.2 M [GdnHCl]. Considering the intensities and shifts of fluorescence spectra, we found a midpoint around 1.5 M in the transition region whose value was similar to 1.47 M [GdnHCl], the transition midpoint obtained by Hlodan and Pain [12]. In addition, in order to normalize the fluorescence intensity data, we measured the fluorescence intensities of *N*-acetyl tryptophan amide (NATA) as an internal standard at the same concentrations with hTNF-α concentrations under various [GdnHCl] (0–4.2 M). As a result, the area and the peak intensity of each NATA fluorescence spectrum did not show any dependence on [GdnHCl] and, therefore, no normalization of the fluorescence spectra was needed (data not shown). From this result, we could confirm that the intensity changes in this [GdnHCl] range definitely originated from the conformational change in hTNF-α rather than the ionic effect conferred by the guanidium ions.

In the detailed analysis, first, fluorescence intensity increased with the increasing concentration of GdnHCl from its native state to 0.6 M and then slightly decreased to 0.9 M, whereas the position of the spectral maximum did not change; the maximum wavelength was about 328 nm at these GdnHCl concentrations. These phenomena may be due to fluorescence quenching induced by the energy transfers among the tryptophans and ultrafast motional dynamics. Second, at above 1.2 M [GdnHCl], a significant change in the spectral maximum was shown. The bands were located at somewhat lower energies compared to those in the low GdnHCl concentration solutions and showed the spectral broadening, implying there were more various couplings between each tryptophan residue and its environment than those in the native state. Finally, in the fully unfolded-state (U) at 4.2 M [GdnHCl], the fluorescence spectrum resembled the typical tryptophan spectrum for the global unfolding of a protein in aqueous solution [22]. Since a fluorescence spectrum of tryptophan residues can reflect the polarity of their surrounding

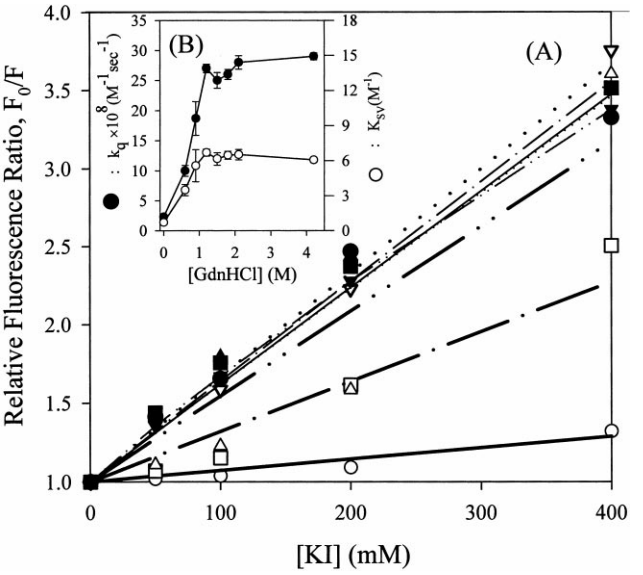

Fig. 3. (A) Stern–Volmer plots for the quenching of steady-state fluorescence intensities of human TNF-α by KI at various GdnHCl concentrations. F_0 and F are the fluorescence intensities in the absence and presence of the quencher, respectively. $Na_2S_2O_3$ (100 μM) as a reductant is also contained to avoid the possible undesired formation of I_3^-. (B) Quenching rate constants (k_q) and the Stern–Volmer quenching constants (K_{sv}) are also plotted to [GdnHCl]. ○, native solution; ———, native fitted; □, 0.6 M GdnHCl solution; – · – · –, 0.6 M fitted; △, 0.9 M GdnHCl solution; – ·· – ·· – 0.9 M fitted; ▽, 1.2 M GdnHCl solution; ···, 1.2 M fitted; ●, 1.5 M GdnHCl solution; ———, 1.5 M fitted; ■, 1.8 M GdnHCl solution, - · - · -, 1.8 M fitted; ▲, 2.1 M GdnHCl solution, - ·· - ·· -, 2.1 M fitted; ▼, 4.2 M GdnHCl solution; ....., 4.2 M fitted.

environments, it is clear that the tryptophan residues are fully exposed to the solvent in this U-state.

On the other hand, when monitored by the secondary structure probe, far-UV CD at various [GdnHCl] (Fig. 2B), very interesting unfolding transition behaviors of TNF-α are shown: the molar ellipticities in the range of 1.2–1.8 M are pronounced by up to 200% of the native molar ellipticity. In addition, the reversed bell-like shape of this transition curve, which is very different from a typical sigmoidal one, is very unusual. The minimal ellipticity in this [GdnHCl] range is comparable to that of the previous acid- or thermal-induced case of human TNF-α that was investigated by Nahri et al. [11,13,14]. According to their results, the conformational property that TNF-α assumes in its molten globule state is regarded as a very interesting one in that while most proteins have native-like second-

ary structures in their molten globule state, TNF-α, all β-sheet protein, is subject to the formation of α-helices in its molten globule or partially denatured state. In the GdnHCl-induced unfolding transition curve monitored by far-UV CD at 220 nm, ellipticities in the transition region (1.2–2.1 M) were negatively pronounced with the turning point of around 1.5 M. This may imply that GdnHCl-induced conformational change can lead to a stable intermediate state, which is very similar in its secondary structure to the molten globule state. When compared to the unfolding transition curve monitored by intrinsic fluorescence, the fundamental difference in the shape indicates that the unfolding transition of TNF-α cannot be viewed from the simple two-state model.

These results about the solvent accessibility were supported, in terms of the fluorescence quenching experiments, by the steady-state spectra in the presence of the quenchers and the lifetime studies in the absence of the quenchers. The fitted lifetime parameters associated with the time resolved fluorescence lifetime experiments are tabulated in Table 1. These results were utilized in deriving the quenching rate constant (k_q) in the fluorescence quenching by KI (refer to Section 3.2) and the anisotropy decay parameters (refer to Section 3.3).

3.2. Fluorescence quenching by potassium iodide (KI)

To check the ionic effects by GdnHCl or KI on this parameter, we measured the fluorescence spectra for TNF-α solutions of several GdnHCl concentrations at a fixed [KI] varying [KCl] in the range of 0–400 mM. No distinguishable change in the shapes and the intensities of the steady-state fluorescence spectra was observed, indicating that the ionic effect offered by GdnHCl or KI was not significant (data not shown). Fig. 3A shows the Stern–Volmer plots which were measured with the different concentrations of GdnHCl at various quencher (KI) concentrations (0–400 mM) and fitted to the Stern–Volmer equation. The mean fluorescence lifetime at each [GdnHCl] in Table 1 was utilized to derive the quenching rate constants (k_q) from Stern–Volmer quenching constants (K_{sv}). Compared with the steady-state spectra in the absence of the quencher, it is confirmed that the presence of the quencher caused no change in the shape of the emission spectra. However, at higher concentrations of iodide (200 mM), the peaks of the emission spectra were blue-shifted to shorter wavelengths (data not shown). These blue-shifted emission spectra upon quenching were due to the remaining unquenched fluorescence of partly buried tryptophan residues [22]. From the quenching studies, no significant quenching was observed in the native state. According to many studies using ionic quenchers like an iodide ion, it is well known that the emission of exposed tryptophan residues are quenched selectively [22,25]. Therefore, the tryptophan residues in the native state are considered to be inaccessible to solvent. In addition, we deduced the effective collisional quenching rate constant (k_q) of 2.33×10^8 M^{-1} S^{-1} with the mean lifetime of 3.1 ns in the native state. On the other hand, the quenching rate constants, which increased from 10×10^8 M^{-1} S^{-1} to 18.7×10^8 M^{-1} S^{-1} with increasing GdnHCl concentration up to 0.9 M, indicated more efficient quenching than that in the native state. In these GdnHCl concentrations ($\sim$0.9 M), compared with the results of native-like solvent exposures from the

Table 1
Fitted parameters associated with the time-resolved fluorescence lifetime measurements under magic angle (54.7°) detection

[GdnHCl]	A_1 (%)	τ_1 (ns)	A_2 (%)	τ_2 (ns)	A_3 (%)	τ_3 (ns)	τ_m (ns)	χ^2
0.0 M	46.7	4.2	29.8	1.8	23.5	0.13	2.8	1.3
0.6 M	63.9	4.0	19.1	1.6	17.0	0.16	2.9	1.3
0.9 M	48.9	4.0	25.8	1.5	25.3	0.13	2.9	1.2
1.2 M	50.5	4.1	26.7	1.5	22.8	0.15	2.5	1.3
1.5 M	32.4	4.9	43.4	1.8	24.1	0.35	2.5	1.2
1.8 M	29.4	5.0	46.3	1.9	24.3	0.43	2.5	1.1
2.1 M	21.5	5.1	49.8	2.2	28.7	0.50	2.3	1.3
4.2 M	32.2	3.9	44.2	1.8	23.6	0.42	2.2	0.96

The non-linear least-square deconvolution fittings were performed using the LIFETIME program. The mean lifetimes were calculated according to the equation, $\tau_m = \Sigma\alpha_i\tau_i/(\Sigma\alpha_i)$.

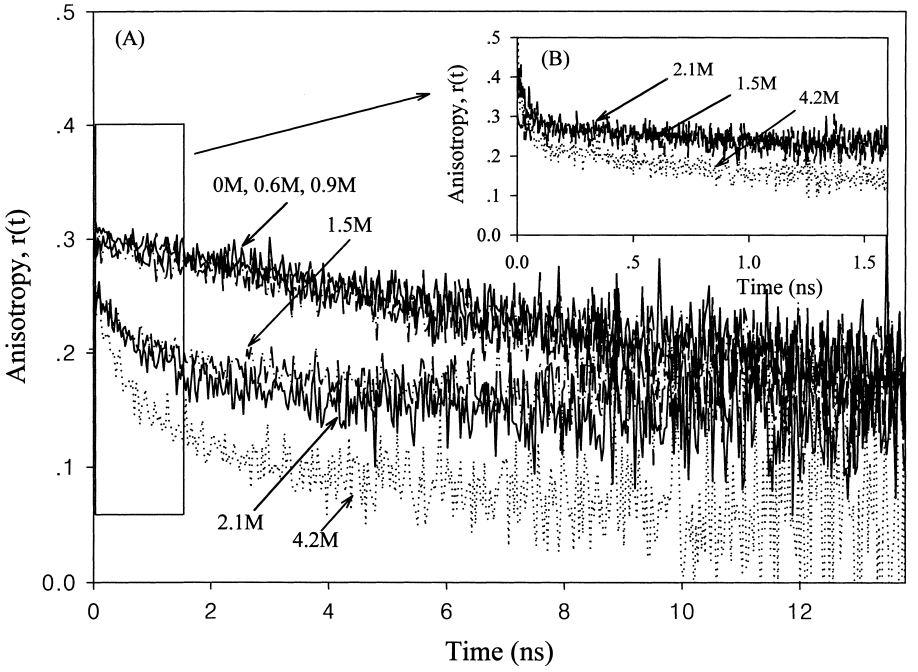

Fig. 4. Fluorescence anisotropy decays of human TNF-α in aqueous phosphate buffer solutions of pH 7.6 at the various GdnHCl concentrations in the 16-ns window (A) and the 2-ns window (B). $r(t)=[I_{\parallel}(t)-g\ I_{\perp}(t)]/[I_{\parallel}(t)+2g\ I_{\perp}(t)]$, where g is a geometric factor and $I_{\parallel}(t)$ is the fluorescence intensity which has the same polarization component as that of excitation radiation and $I_{\perp}(t)$ is the orthogonally polarized fluorescence intensity to that of the excitation field.

steady-state spectra in the absence of the quencher, it is suggested that the increased quenching rate constants were due to the less dense surface at which an iodide ion can quench tryptophan fluorescence substantially. At above 1.2 M [GdnHCl], the level of the quenching was significantly higher than that in the native state, and the deduced quenching rate constants using available lifetime data were in the range of $25–29\times10^{8}$ M^{-1} S^{-1}. These efficient quenching results indicate that the tryptophan residues in this concentration range are more exposed to the solvent. Since the charged quenchers do not readily penetrate the hydrophobic interior of proteins, the iodide quenching behavior demonstrates that the loosely packed intermediates, which have largely exposed tryptophan residues above 1.2 M [GdnHCl], are present. Overall, the transition from the steep to the slow slope in the quenching rate constants exists around 1.2 M [GdnHCl], indicating that it can be the beginning region of structural change. When we consider all of the transition curves monitored by various spectroscopic methods including the steady-state fluorescence, far-UV CD, and fluorescence quenching by KI, the results related to the conformational changes at the range of 1.2–2.1 M [GdnHCl] can be summarized as follows. In this [GdnHCl] region, the local structures around Trp residues were immersed into polar environments where Trp residues became largely solvent-accessible. This conformational transition also concurrently occurred with the large changes in the secondary structure as shown from the negatively pronounced molar ellipticity in this [GdnHCl] region at 222 nm.

3.3. Picosecond time-resolved fluorescence anisotropy decay measurements

The unfolding pathway of this protein was also investigated by picosecond time-resolved fluorescence anisotropy experiments. The measured anisotropy decay curves are shown in Figs. 4 and 5. The fitted parameters including the rotational correlation times (τ_1, τ_2) and the corresponding amplitudes (r_{01}, r_{02}), anisotropic plateau values (r_{∞}), and the chi-square values (χ^2) of the fits are listed in Table 2. Such time-resolved fluorescence anisotropy decay was measured in order to obtain specific information on the rotational dynamics which could be related not

only to local tryptophan mobility, but also to the entire protein motion, which occur from nanosecond to picosecond time scale [22–24].

In order to help in assigning the experimental rotational correlation times of the native and the unfolded states to their dominant multimeric states, the modified Debye–Stokes–Einstein hydrodynamic theory was used [27,28]. The rotational correlation times of the native trimer, dimer, and monomer were calculated with a generalization toward the asymmetric ellipsoid. When this theory is applied, the stick boundary condition is relevant for proteins in an aqueous solution [29]. The general solution of this model with three different molecular axial lengths assuming the absorption and emission transition dipoles along the longest molecular axis is as follows [27,28].

$$r(t) = 0.3(2/3 + G)\exp[-(6D-2\Delta)t]+$$
$$0.3(2/3-G)\exp[-(6D + 2\Delta)t] \quad (1)$$

where

$$D = (D_a + D_b + D_c)/3$$

$$\Delta = (D_a^2 + D_b^2 + D_c^2 - D_aD_b - D_bD_c - D_cD_a)^{1/2} \quad (2)$$

$$G = (D_a - D)/\Delta.$$

Here the rotational diffusion constant D_i is given by

$$D_i = kT/f_i. \quad (3)$$

The frictional coefficients f_i for the stick boundary condition can be obtained from the evaluation of elliptical integrals pertinent to the dimensions of the asymmetric ellipsoid and the corresponding boundary condition. To get the information on the dimensions of each multimeric state, we referred to van der Waals' dimensions modeled from the atomic coordinates of an X-ray crystallographic structure of hTNF-α which was processed with the computer program, QUANTA [10]. In the trimeric case, the ellipsoid has the dimensions of 65×52×52 Å. The calculated overall rotational correlation time is 24.5 ns. For the dimeric and the monomeric cases, van der Waals' dimensions are 65×44×30 Å and 65×30×29 Å, respectively. For these two asymmetric cases, two rotational correlation times were derived. The values were 15.6 and 11.3 ns for the dimeric case, and those in the monomeric case were both the same as 8.9 ns.

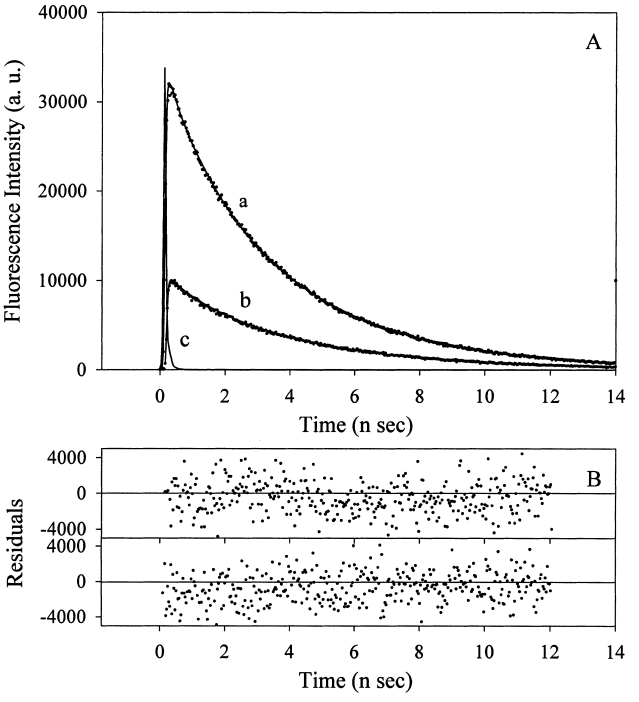

Fig. 5. (A) The fluorescence intensity decays and the fitted lines of TNF-α at 0 M [GdnHCl] for the horizontal (a) and the vertical (b) polarization components are in time-resolved fluorescence anisotropy measurements using the TCSPC detection system. The excitation wavelength and the emission wavelength were 295 and 330 nm, respectively. The protein concentration was about 0.125 mg/ml in a 50 mM sodium phosphate buffer of pH 7.6 at 20°C. A typical half-width of the laser pulse was about 2–3 ps. The FWHM of the instrumental response function (c) was about 60 ps. The observed vertical and horizontal fluorescence intensity decay curves were analyzed simultaneously through the iterative non-linear least-squares deconvolution fitting routine of the LIFETIME program. The anisotropy decay data at the other GdnHCl concentrations were fitted in the same manner. The time-per-channel in the multi-channel analyzer (MCA) was about 31.3 ps/channel. (B) The residuals of the lifetime fittings are shown (top, vertical components; bottom, horizontal components).

In the native state, we observed the single-exponential decay with the rotational correlation time of 22 ns. This value is consistent with an earlier experimental study [11] and similar to that of the trimeric case in our hydrodynamic calculations. Therefore we could characterize it as the overall tumbling time for the whole protein, not the polypeptide segmental mobility. These observations imply that the environment

Table 2
(A) Fitted parameters for fluorescence anisotropy decays in 16 ns window and (B) fitted parameters in 2 ns window

[GdnHCl]	r_0	r_{01}	r_{02}	τ_1 (ns)	τ_2 (ns)	r_∞	χ^2
(A) 16-ns window							
0.0 M	0.30		0.30		22	0	1.4
0.6 M	0.31		0.31		24	0	1.2
0.9 M	0.28		0.28		25	0	1.2
1.5 M	0.25	0.03	0.05	0.32	2.0	0.17	1.0
2.1 M	0.24	0.07	0.03	0.89	6.0	0.14	1.1
4.2 M	0.25	0.07	0.10	0.39	2.3	0.08	1.3
(B) 2-ns window							
1.5 M	0.28		0.08		1.7	0.19	0.98
2.1 M	0.39	0.12	0.13	0.03	2.8	0.15	1.1
4.2 M	0.39	0.18	0.12	0.03	1.5	0.10	1.0

For more precise data at the GdnHCl concentrations (1.5, 2.1 and 4.2 M), the fitted anisotropy values should be referred by the data which were collected with the 2-ns window. The anisotropy decay function is set to $r(t) = r_{01}\ \exp(-t/\tau_1) + r_{02}\ \exp(-t/\tau_2) + r_\infty$ and r_0 (initial anisotropy) $= r_{01} + r_{02} + r_\infty$.

of tryptophan residues is very rigid in this state. From the fitted values in Table 2, as the concentration of GdnHCl increases up to 0.9 M, the rotational correlation times become slower than that of the native state by about 20% with a good single exponential fitting. These results imply that the protein is slightly swelling as a trimer, and the local mobility of tryptophan residues does not exist in our time scale. In contrast to this behavior, the anisotropy decays between 1.5 and 2.1 M [GdnHCl] could not be fitted with a single exponential. We have obtained two anisotropy correlation times of hundreds of picoseconds and 2–6 ns. Since these time constants are much faster than the overall tumbling time of the monomer from the hydrodynamic calculations, it is plausible to say that they represent the motions of the tryptophan side chains and polypeptide segments. And the very large anisotropic plateau values (r_∞) in the anisotropy measurements between 1.5 and 2.1 M [GdnHCl] raise the possibility that human TNF-α unfolds through the formation of aggregates whose correlation time is too long to be detected. These interpretations of the aggregated state were also recently reported for the GdnHCl-induced proteins [20,21,30]. Therefore, we suggest that the anisotropic plateau values (r_∞) in these states may represent both the extent of aggregation and restricted motions. Finally, we have obtained two correlation times also in the U-state, and it is clear that these values are within the range typically found for a peptide chain in random coil conformation and the relatively free rotation time of tryptophan obtained from other denatured proteins in the earlier studies [11,20,22,30–32]. In particular, it is interesting to note that the anisotropy did not decay back to zero in the U-state as well as 1.5–2.1 M [GdnHCl]. This phenomenon is likely due to the hindrance of the anisotropic motion, which comes from aggregated, long polypeptide chains [30].

By the time-resolved fluorescence anisotropy, we could observe the motional dynamics of the internal side chains. Therefore, combining the fluorescence anisotropy results with the solvent accessibility known by the steady-state fluorescence and the iodide quenching experiments, we observed the aggregated and loosely packed structures showing the high level solvent accessibility of tryptophan residues in this GdnHCl concentration region.

However, the previously mentioned initial anisotropy values (r_0) between 1.5 and 4.2 M [GdnHCl] in a 16-ns window were in the range of 0.24–0.25, which were smaller than the values (0.27–0.35) observed in the case of tryptophan in rigid environments [20,33]. Therefore, in order to obtain more precise information on the fast, unresolved motion and also to confirm the two exponential decay behaviors in the 16-ns window, we performed picosecond time-resolved fluorescence anisotropy measurements in the 2-ns window. Also, the values listed in Table 2 are fitted parameters of anisotropy decays in the 2-ns window. A detailed analysis of the fitted data is as follows. In 1.5 M [GdnHCl], a 1.7 ns correlation time with the anisotropic plateau value (r_∞) was observed instead of two correlation times in the previous 16-ns window. Therefore, we can consider that the lack of internal motion of buried tryptophans still exists due to the densely packed structure. This is unlike the other concentrations of 2.1–4.2 M [GdnHCl] which showed two fast correlation times representing the free rotations of the Trp side chains and segmental mobility for the fast decay of 30 ps and the slow decay of 1.5–2.8 ns, respectively, with the anisotropic plateau values corresponding to the very slow rotation of aggregates or

unresolved restricted anisotropic motions. In addition, since the initial anisotropy (r_0) in the 1.5 M GdnHCl solution is smaller than those in the other concentrations (2.1–4.2 M [GdnHCl]), it is likely that unresolved fast motion or energy transfer among the tryptophans may exist at 1.5 M [GdnHCl].

In recent years, it has been suggested that both short- and long-range interactions in the conformation of this protein are important [13,14]. Therefore, we could say that the environmental variation of the tryptophans was due to the change in both the short and the long range interactions followed by a larger disruption of the tertiary structure between 1.5 and 2.1 M [GdnHCl]. Comprehensively, this study reveals that the tryptophan side chains do not have any rotational degree of freedom from a native state to 0.9 M [GdnHCl], whereas from 1.5 to 4.2 M [GdnHCl], the protein unfolds with the existence of the hydrated free rotations of tryptophans and the segmental mobility as well as the aggregated states inducing the large anisotropic plateau values (r_∞).

4. Conclusions

In this study, we have shown the nature of the GdnHCl-induced dynamic equilibrium unfolding pathway of human TNF-α with the steady-state fluorescence spectroscopy and the picosecond time-resolved fluorescence anisotropy decay measurements. From the native state to 0.9 M [GdnHCl], we have obtained one rotational correlation time corresponding to the overall tumbling time of a whole trimeric protein which showed a rigid environment for all the tryptophan residues and the absence of any polypeptide segmental mobility near the tryptophan residues. At about 1.2–1.5 M [GdnHCl], tryptophans which were inaccessible to the iodide in the native state became highly accessible. Human TNF-α had a high degree of internal motion and appeared to aggregate to a great extent due to its increased hydrophobicity similar to the case of the thermal-induced unfolding study [13]. In particular, the very short rotational correlation times (30 ps) which appeared in 2.1 and 4.2 M [GdnHCl] represented more hydrated tryptophan environments than those in 1.5 M [GdnHCl], with more increased exposure to the solvent.

In conclusion, we suggest the elucidative unfolding pathway as follows. (1) The native trimer unfolds as a slightly swelled trimer maintaining its internal structure up to 0.9 M [GdnHCl]. (2) It then associates into aggregates containing partially folded structures which begin to show the internal degree of freedoms, such as the mobility of polypeptide segments or tryptophan side chains around 1.5 M [GdnHCl]. (3) At 2.1 M [GdnHCl], the tryptophan residues become more highly accessible to the solvent environment while maintaining the partially folded structures as those in 1.5 M [GdnHCl]. (4) Finally, a fully unfolded structure like an extended random coil conformation is formed in 4.2 M [GdnHCl].

Since at present very little information exists about the possible transient species which undergo the unfolding pathway, an interesting question that requires further study is how the conformation of human TNF-α in each state precisely influences kinetic photophysics and mobility of tryptophan residues. However, since tryptophan residues in wild type human TNF-α are located at two positions (Trp-28, Trp-114), these observations could not be explained in terms of each tryptophan residue. Therefore, an investigation of human TNF-α which has only one (Trp-114) of two tryptophan residues which has replaced to Phe-114 may be needed to avoid the complexity of the interpretation. Thus, dynamic or kinetic fluorescence studies of the mutant (W114F) human TNF-α protein as well as the contribution of this substituted Trp residue to the thermodynamic stability of the protein are in progress.

Acknowledgements

This research was supported by a grant from the G7 Project and the National Creative Research Initiatives (D. Kim) of the Ministry of Science and Technology, and Y.-R. Kim thanks for the partial support from CRM-KOSEF grant (98K3-0302-01-01-3), Republic of Korea.

References

[1] T.E. Creighton, J. Phys. Chem. 89 (1985) 2452–2459.

[2] P.S. Kim, R.L. Baldwin, Annu. Rev. Biochem. 59 (1990) 631–666.
[3] H. Christensen, R.H. Pain, in: R.H. Pain (Ed.), Mechanisms of Protein Folding, Oxford University Press, Oxford, 1994.
[4] T.E. Creighton, Proteins: Structures and Molecular Properties, 2nd edn., W.H. Freeman, New York, 1992.
[5] E.A. Carswell, L.J. Old, R.L. Kassel, S. Green, N. Fiore, B. Williamson, Proc. Natl. Acad. Sci. USA 72 (1975) 3666–3670.
[6] W. Fiers, FEBS Lett. 285 (1991) 199–212.
[7] R. Beyaert, W. Fiers, FEBS Lett. 340 (1994) 9–16.
[8] P.F. Wingfield, R.H. Pain, S. Craig, FEBS Lett. 211 (1987) 179–184.
[9] E.Y. Jones, D.I. Stuart, N.P.C. Walker, Nature 338 (1989) 225–228.
[10] M.J. Eck, S.R. Sprang, J. Biol. Chem. 264 (1989) 17595–17605.
[11] R. Hlodan, R.H. Pain, FEBS Lett. 343 (1994) 256–260.
[12] R. Hlodan, R.H. Pain, Eur. J. Biochem. 231 (1995) 381–387.
[13] L.O. Nahri, J.S. Philo, T. Li, M. Zhang, B. Sonal, T. Arakawa, Biochemistry 35 (1996) 11447–11453.
[14] L.O. Nahri, J.S. Philo, T. Li, M. Zhang, B. Sonal, T. Arakawa, Biochemistry 35 (1996) 11454–11460.
[15] J. Erhardt, H. Dirr, Eur. J. Biochem. 230 (1995) 614–620.
[16] M.A. Sherman, J.M. Beechem, M.T. Mas, Biochemistry 34 (1995) 13934–13942.
[17] J.M. Beechem, M.A. Sherman, M.T. Mas, Biochemistry 34 (1995) 13943–13948.
[18] V.N. Uversky, O.B. Ptitsyn, J. Mol. Biol. 255 (1996) 215–228.
[19] M.R. Eftink, R. Isonescu, G.D. Ramsay, C.Y. Wong, J.Q. Wu, A.H. Maki, Biochemistry 35 (1996) 8084–8094.
[20] R. Swaminathan, U. Nath, J.B. Udgaonkar, N. Periasamy, G. Krishnamoorthy, Biochemistry 35 (1996) 9150–9157.
[21] M.M.S. Pino, A.R. Fersht, Biochemistry 36 (1997) 5560–5565.
[22] J.R. Lakowitcz, Principles of Fluorescence Spectroscopy, Plenum Press, New York, 1983.
[23] J.M. Beechem, L. Brand, Annu. Rev. Biochem. 54 (1985) 43–71.
[24] P. Wu, L. Brand, Anal. Biochem. 218 (1994) 1–13.
[25] B. Somogyi, S. Papp, A. Rosenbery, I. Seres, J. Matko, G.R. Welch, P. Nagy, Biochemistry 24 (1985) 6674–6679.
[26] M.Y. Lee, D. Kim, J. Opt. Soc. Kor. 5 (1994) 90–99.
[27] T.J. Chuang, K.B. Eisenthal, J. Chem. Phys. 57 (1972) 5094–5102.
[28] Y.-R. Kim, R. Hochstrasser, J. Phys. Chem. 96 (1992) 9595–9597.
[29] C.M. Hu, R. Zwanzig, J. Chem. Phys. 60 (1974) 4354–4357.
[30] R. Swaminathan, N. Periasamy, J.B. Udgaonkar, G. Krishnamoorthy, J. Phys. Chem. 98 (1994) 9270–9278.
[31] L.X.Q. Chen, J.W. Petrich, G.R. Fleming, Chem. Phys. Lett. 139 (1987) 55–61.
[32] C. Rischel, P. Thyberg, R. Rigler, F.M. Poulsen, J. Mol. Biol. 257 (1996) 877–885.
[33] M.R. Eftink, I. Gryczynski, W. Wiczk, G. Laczko, J.R. Lakowicz, Biochemistry 30 (1991) 8945–8953.